BJP British Journal of Pharmacology

DOI:10.1111/bph.12682
www.brjpharmacol.org

RESEARCH PAPER

Regulation of ACh release from guinea pig bladder urothelial cells: potential role in bladder filling sensations

L M McLatchie, J S Young* and C H Fry

Department of Biochemistry and Physiology, FHMS, University of Surrey, Guildford, UK

Correspondence
Linda McLatchie, Department of Biochemistry and Physiology, FHMS, University of Surrey, Guildford GU2 7XH, UK. E-mail: l.mclatchie@surrey.ac.uk

*Present address: School of Pharmacy & Biomedical Sciences, University of Portsmouth, Portsmouth, PO1 2DT.

Keywords
non-neuronal ACh; urothelial cells; ATP; anti-muscarinic agents; CFTR; urinary bladder

Received
1 October 2013
Revised
25 February 2014
Accepted
1 March 2014

BACKGROUND AND PURPOSE
The aim of this study was to quantify and characterize the mechanism of non-neuronal ACh release from bladder urothelial cells and to determine if urothelial cells could be a site of action of anti-muscarinic drugs.

EXPERIMENTAL APPROACH
A novel technique was developed whereby ACh could be measured from freshly isolated guinea pig urothelial cells in suspension following mechanical stimulation. Various agents were used to manipulate possible ACh release pathways in turn and to study the effects of muscarinic receptor activation and inhibition on urothelial ATP release.

KEY RESULTS
Minimal mechanical stimulus achieved full ACh release, indicating a small dynamic range and possible all-or-none signal. ACh release involved a mechanism dependent on the anion channel CFTR and intracellular calcium concentration, but was independent of extracellular calcium, vesicular trafficking, connexins or pannexins, organic cation transporters and was not affected by botulinum-A toxin. Stimulating ACh receptors increased ATP production and antagonizing them reduced ATP release, suggesting a link between ACh and ATP release.

CONCLUSIONS AND IMPLICATIONS
These results suggest that release of non-neuronal ACh from the urothelium is large enough and well located to act as a modulator of ATP release. It is hypothesized that this pathway may contribute to the actions of anti-muscarinic drugs in reducing the symptoms of lower urinary tract syndromes. Additionally the involvement of CFTR in ACh release suggests an exciting new direction for the treatment of these conditions.

Abbreviations
4-DAMP, 1,1-dimethyl-4-diphenylacetoxypiperidinium iodide; BTX, botulinum toxin; CFTR, cystic fibrosis transmembrane conductance regulator; CK20, cytokeratin 20

Introduction

The bladder urothelium is exquisitely designed to provide a barrier to the urine contained within the bladder while also being a sensory epithelium, both releasing and responding to numerous chemical transmitters. There is now good evidence that ACh is one of these transmitters, as the urothelium has been shown to contain all the enzymes required to synthesize

© 2014 The British Pharmacological Society

ACh (Yoshida *et al.*, 2006; Hanna-Mitchell *et al.*, 2007; Lips *et al.*, 2007), non-neuronal ACh release is reduced following urothelium removal (Yoshida *et al.*, 2004; 2006) and cultured urothelial cells have been demonstrated to release ACh (Hanna-Mitchell *et al.*, 2007). This non-neuronal ACh release only accounts for about 1–2% of the total bladder ACh in people below 65, but rises to 5% or more with age (Yoshida *et al.*, 2004). Given its small contribution, the role of non-neuronal ACh is unclear but it may regulate bladder tone and contribute to overactive bladder contractions because anti-muscarinic drugs are most effective during the storage phase when neuronal release is low (Yoshida *et al.*, 2004; Andersson, 2011). An autocrine signalling role is also possible, regulating its own release (Hanna-Mitchell *et al.*, 2007) or that of other mediators such as ATP or NO. Functional muscarinic and nicotinic receptors have been demonstrated in cultured urothelial cells and a link to ATP release demonstrated in guinea pig bladder strips (Beckel *et al.*, 2006; Hanna-Mitchell *et al.*, 2007; Kullmann *et al.*, 2008; Young *et al.*, 2012).

The mechanism of urothelial cell ACh release is unknown, although it is probably non-vesicular as it is insensitive to brefeldin A (BFA) and also urothelial cells lack a vesicular ACh transporter (Hanna-Mitchell *et al.*, 2007). In human placenta, organic cation transporters OCT1 and OCT3 are implicated in ACh release as OCT1 transported ACh when expressed in *Xenopus* oocytes (Wessler *et al.*, 2001; Lips *et al.*, 2005; nomenclature follows Alexander *et al.*, 2013). Both OCT1 and OCT3 are present in mouse and human urothelium, although neither has been demonstrated to be involved in ACh release in bladder (Lips *et al.*, 2007).

Here, we used freshly isolated guinea pig urothelial cells to characterize the mechanism of ACh release. Using freshly isolated rather than cultured cells allowed less time for morphological (Woodman *et al.*, 2011) and functional changes and also reduced the possibility of contamination from faster growing non-urothelial cells, while still utilizing an almost pure population of known cellular composition, not possible with whole tissue. We used a range of agents to investigate possible ACh release pathways and also investigated the effects of ACh on ATP release from urothelial cells.

The results presented here show that ACh is released from urothelial cells when mechanically stimulated, by a novel route that differs from that of ATP. It is hypothesized that this ACh controls ATP release and that this pathway may contribute to the actions of anti-muscarinic agents in reducing symptoms of lower urinary tract syndrome and painful bladder syndrome. Preliminary findings were presented to the International Continence Society (Fry and McLatchie, 2013).

Materials and methods

Cell isolation

All animal care and experimental procedures complied with the UK Animals, Scientific Procedures Act 1986 and European Communities Council Directive 86/09/EEC and were approved by the ethical committee of Faculty of Health and Medical Sciences, University of Surrey All studies involving animals are reported in accordance with the ARRIVE guidelines for reporting experiments involving animals (Kilkenny *et al.*, 2010; McGrath *et al.*, 2010). A total of 133 animals were used in the experiments described here. Male guinea pigs (Dunkin-Hartley; 400–600 g) were killed by cervical dislocation Bladders were immediately excised, the mucosa removed by blunt dissection and incubated at 37°C with trypsin-EDTA (0.5 g·L^{-1} trypsin, 0.2 g·L^{-1} EDTA, Sigma, Poole, Dorset, UK) in PBS for approximately 40 min. Urothelial cells were released by gentle titration, washed with Tyrode's solution, a sample taken and counted and the cell suspension incubated in Eppendorf tubes at a known density. By varying the length of incubation with trypsin-EDTA, it was possible to obtain a population containing varying percentages of the three subtypes of urothelial cells; shorter incubation having more of the larger cells for example. For the study shown in Figure 3C, two extreme populations were obtained, with a high and a low percentage of the larger umbrella cells. These were then diluted to give the same number of these types of cells per mL, but obviously with a different total cell density and then mixed in different ratios to give the intermediate densities.

When used, one of BFA (10^{-5} g·mL^{-1}),the inhibitor of the cystic fibrosis transmembrane conductance regulator, $CFTR_{inh}$-172 (3×10^{-8} – 7.5×10^{-5} M), quinine (10^{-4} M), botulinum toxin-A (BTX-A; 4U and 10U) was added at this stage. Carbachol (10^{-5} M) and 1,1-dimethyl-4-diphenylacetoxypiperidinium iodide (4-DAMP; 5×10^{-7} M) were added just prior to measurement of transmitter release and carbenoxolone (5×10^{-4} M), 35–50 min before testing. Methoctramine was either added at the start of incubation (for experiments with carbachol as well) or just prior to measuring transmitter release for the other experiments (10^{-8}–10^{-5} M). Appropriate vehicle/dilution controls were used in all cases. All experiments were carried out at room temperature.

Cell counting

All cell counts used an improved Neubauer haemocytometer stage. The percentage of viable cells was calculated by the proportion excluding Trypan blue (0.4 % solution) added to a 10 µL sample of the cell suspension. All cell preparations were counted and the percentage excluding Trypan blue measured from a sample taken before using the rest of the population. The percentage of large-, medium- and small-sized cells was estimated visually from two separate counts of each population. In five preparations cell diameter, x, was measured and plotted as a histogram in 1 µm bins. Each histogram was positively skewed and optimal fits were obtained by fitting them to three Gaussian distributions (equation 1), that is, the variance of the fit was significantly reduced with three distributions using Fisher's exact test.

$$n(x) = \frac{1}{\sigma\sqrt{2\pi}} \exp\left(-\frac{(x-\bar{x})^2}{2\sigma^2}\right) \quad (1)$$

Where n = number of cells, $\bar{x}$ and σ are the mean and standard deviation of an individual distribution. Histograms were initially fitted to the smallest bin sizes (8–12 µm) to generate the first distribution and the residuals treated in a similar way to generate distributions for intermediate and the largest cell populations. Total cell number and the proportion in each population were calculated for each cell preparation.

Immunohistochemistry

Epitope labelling on cells was done at room temperature. Suspensions were fixed with 2% paraformaldehyde for 6 min and then washed twice in PBS (40× *g*, 6 min each time). PBS with 1% BSA and 0.2% Triton was added for at least an hour followed by the primary antibody to cytokeratin 20 (CK20) (mouse monoclonal anti-KRT20; Sigma WH0054474M1,) at 1:100 for 1 h. Following washing, secondary antibody (Alexa-Fluor 488 goat anti-mouse, Invitrogen, Renfrew, Glasgow, UK, A10680 at 1:500) was added for 45 min and the cells washed and viewed using confocal microscopy.

CFTR immunohistochemistry used the same protocol except that 12 μm sections of whole bladder were used, paraformaldehyde was only applied for four minutes, 0.5% triton and 3% BSA were used and incubation with primary antibody was 24 h at 4°C (Abcam, Cambridge, UK, anti-CFTR ab2784, mouse monoclonal, 1:50). Vectashield (Vector Labs, Peterborough, UK) was used to mount sections before viewing.

ACh and ATP stimulation and measurement

Cell suspensions (45 μL samples) were stabilized in Tyrode's solution (below) for at least 90 min, after which a mechanical shear stress was applied by pipetting 20 μL of suspension up and down at a constant speed, using the same pipette and type of pipette tip (see Supporting Information Appendix S1 for more details). ACh was measured, using an Amplex®Red ACh/acetyl cholinesterase assay kit (Invitrogen, A12217), from 20 μL samples taken immediately following five such actions (except Figure 2A) and rapidly frozen until required. These samples were then mixed with 20 μL of the reaction mixture made as given in the instructions for the kit except for the smaller volume used. Fluorescence was measured at 590 nm following excitation at 544 nm using a BMG FLUOstar Omega multi-mode (BMG FLUOstar, Promega, Southampton, UK) plate reader. ACh standards were included in all plates (3×10^{-8}–3×10^{-4} M) and fluorescence increase with concentration as shown in Figure 2A. Stimulated ATP release was measured four minutes after shear stress (1 min for Figure 2B) using a luciferin-luciferase assay (FL-AAM, Sigma; GloMax 20/20; Promega) with either a 1 in 2 or a 1 in 10 dilution. Four minutes was used as the ATP level was found to be stable over this period and it was more convenient and allowed tubes from different treatment groups to be processed in parallel. Luminescence was a linear function of concentration on a calibration log-log plot over the range 1×10^{-10}–10^{-6} M. The different number of pipetting stimuli of 5 and 50 stimuli for ACh and ATP, respectively, were each chosen to be maximal (see Figure 2C,D) to minimize the effects of any small variations in the speed or strength of the stimulation. In all experiments, multiple tubes were used for each treatment and averaged to give a single *n* value to reduce variability from errors in stimulus reproducibility still further. The use of multiple tubes for each treatment should also have randomized any errors in stimulus reproducibility between groups and thereby would not be expected to have been responsible for any of the differences seen between groups. Five pipetting stimuli had no significant effect on cell viability as Trypan blue exclusion was not significantly changed as compared with controls (89.3 ± 1.4% compared with control of 88.6 ± 1.8%, $n = 5$). Fifty stimuli did cause a small increase in Trypan blue uptake but his would have been common to both test and control groups and was therefore unlikely to have caused the differences seen (81.6% as compared with control of 86.1% cells excluded Trypan blue, $n = 8$).

Solutions

Tyrode's solution (mM: NaCl 118, $NaHCO_3$ 24, KCl 4.0, $MgCl_2$ 1.0, NaH_2PO_4 0.4, glucose 6.1, sodium pyruvate 5.0, gassed with 95% O_2/5% CO_2) with no added calcium was used for all experiments except Figure 3D where either 1.8 mM $CaCl_2$ was added as indicated, or low sodium solution was used. Low sodium solution was made as for Tyrode's solution but with Tris substituted for NaCl. This solution had a calculated sodium concentration of 29 mM instead of 147.4 mM. During cell isolation PBS and trypsin-EDTA were used.

Data analysis

Mean ACh/ATP release values, when normalized to cell surface area, were not indistinguishable from a normal distribution by a Kolmogorov–Smirnov test. Data are therefore expressed as mean values ± SEM. ATP or ACh release in the presence of an agent is expressed as a percentage of its paired vehicle control. A paired Student's *t*-test was used to compare ACh or ATP release in the presence of each agent with its time-matched vehicle control: the null hypothesis was rejected at $P < 0.05$. In all experiments, *n* number indicates the number of animals except those in Figures 3A,B where separate populations with different distributions of the three sub-types of cells or a different total density were included from the same animal.

Materials

BFA, carbenoxolone, $CFTR_{inh}$-172, quinine, and carbachol were supplied by Sigma; 4-DAMP was from Tocris and BTX-A from Allergan.

Results

Urothelial cell characterization

The isolated guinea pig urothelial cells (Figure 1A) ranged in diameter from 7 to 40 μm and had a frequency size distribution that was well fitted by three Gaussian distributions (Figure 1B) called in ascending size basal, intermediate and umbrella populations. From five sample preparations, the mean population diameters were 11.8 ± 0.4, 18.0 ± 0.7 and 25.7 ± 1.1 in the proportions 0.37 ± 0.05, 0.41 ± 0.01 and 0.22 ± 0.05 μm respectively. Thus, the larger cells were significantly less numerous than the other two cell types in these isolated populations. These distributions are likely to be determined by the length of trypsin EDTA incubation as the percentage of the larger cell group could be increased for example by reducing the incubation time, and therefore cannot be used to assess the relative numbers of the different cell types *in vivo*. Cell viability was confirmed as >80% for all isolations used by Trypan blue exclusion: 90.2 ± 0.4% ($n = 121$). Immunostaining for CK20 labelled 95 ± 2% of cells from four sample preparations, indicating their urothelial origin (Figure 1C).

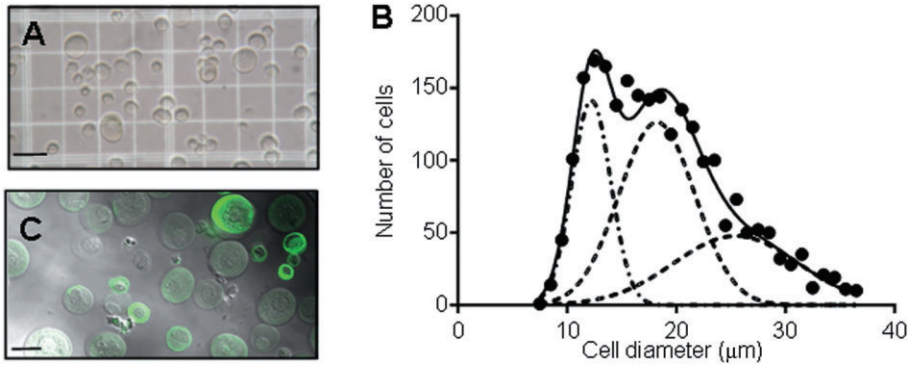

Figure 1

The population of isolated urothelial cells. (A) Isolated urothelial cells as viewed to count and differentiate sub-populations, bar is 50 μm. (B) Frequency distribution of cell diameters of 2399 cells from five populations fitted with three Gaussians distributions (see Methods). Envelope shows the sum of these three fits. (C) Cells labelled with antibody to CK20 to show their urothelial origin, bar is 20 μm.

Comparison of ACh and ATP release

Mechanical stimulation released both ACh and for comparison, ATP. ACh release was measured using an Amplex®Red ACh/acetyl cholinesterase assay kit (Invitrogen). Figure 2A shows the sensitivity of this assay, which had a range from about 0.3 to 300 μM. The experiments described here utilized the lower end of this curve with maximal ACh release reaching about 20 μM. ACh release from 24 tubes from a single experiment is shown in Figure 2B. ACh release can be seen to significantly increase following pipetting the solution up and down (pipetting action) above that in the absence of stimulation. Maximal ACh release was achieved after a relatively small number of pipetting actions, which is shown more clearly in Figure 2C that compares the increase in ACh release above baseline from 10 such experiments. This pattern of release differed to that for ATP, which was not maximal until about 50 pipetting stimuli and was also about twofold lower than that for ACh (Figure 2D). Given the high sensitivity of the ACh release, the actual baseline ACh release is likely to be smaller than these data imply, as there would be stimulation during sampling itself. With ATP release, it was estimated that baseline was overestimated by about 15% due to sampling stimulation by taking multiple samples from the same tube (data not shown). The high sensitivity with ACh prevented this type of calculation but we would predict an even larger effect. Comparison of maximal total ACh and ATP released without subtraction of baseline values indicates levels of as much as five times more ACh than ATP.

Quantification of ACh release

The amount of ACh release following maximal stimulation was measured and is plotted in Figure 3A as a function of total cell surface area for each individual population. This was calculated using the total cell number and percentages of each sub-type of cell in that population and assuming that all the cells were spherical. It can be seen clearly that the amount of ACh release increases with the total surface area. To determine the amount and range of ACh release more clearly, these data are presented in Figure 3B as a frequency histogram. The average ACh release from these individual calculations was 8.3 ± 0.3 moles^{-18}·μm^{-2}: which is equivalent to about 3 μmoles·g^{-1} of cells (assuming a specific density of 1 g·cm^{-3}).

To try to discriminate between the release properties of different urothelial cell populations, the number of large diameter cells was kept constant at 2.25×10^4 mL^{-1} while total cell density was varied in different samples from a single isolation (see methods for details). From the gradient and intercept, respectively, of linear regressions fitted to sets of these data, such as is shown in Figure 3C, ACh production was calculated at 11.7 ± 2.4 moles^{-18}·μm^{-2} (n = 6) for the two smaller cell populations and 7.0 ± 7.7 moles^{-18}·μm^{-2} (n = 6), for the larger cell population. These values are all well within the range shown in Figure 3B suggesting that the three groups of cells all contribute a similar amount of ACh release per unit area.

The effect of calcium on ACh release was investigated in Figure 3D. Addition of 1.8 mM external calcium had no significant effect on ACh release; however, increasing intracellular calcium by perfusing the cells with low sodium solution caused a significant reduction in ACh release to 43 ± 3% of control (P = 0.0001, n = 11). This effect was reversed by incubating the cells in BAPTA-AM to chelate the internal calcium consistent with it being caused by the rise in intracellular calcium.

Pathways involved in ACh release

To study the mechanism of ACh release, cells were treated with compounds designed to block different potential release pathways in turn. The results are summarized in Figure 4A. Each bar shows the amount of ACh release following that treatment expressed as a percentage of its respective paired vehicle control. BFA and BTX were both without significant effect on stimulated ACh release suggesting a non-vesicular mechanism of release. Carbenoxolone, which blocks connexins and pannexins at the concentration used, was also without effect. Organic cation transporters OCT1, OCT2 and OCT3 have all been demonstrated to be blocked by quinine with IC_{50} values between 0.9 and 14 μM (Koepsell *et al.*, 1998). In the current experiment however, quinine at 100 μM was without significant effect on ACh release suggesting that

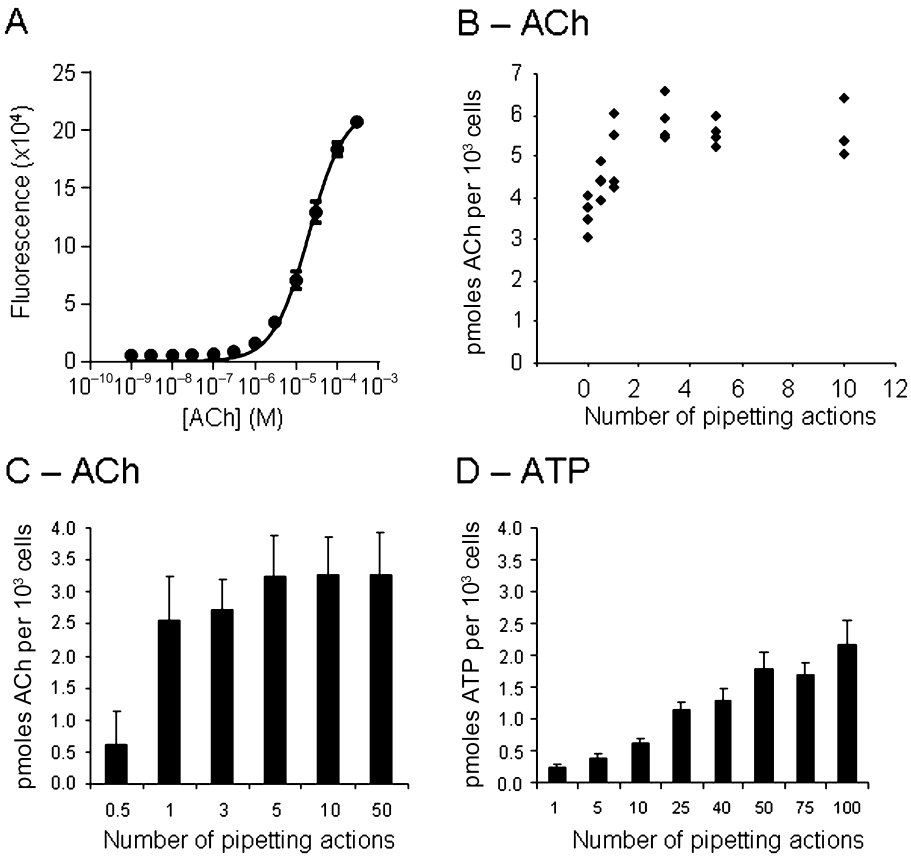

Figure 2

Urothelial cells release ACh and ATP. (A) Standard curve for the ACh assay showing the dynamic range (approximately 0.3–300 μM). (B) ACh release from 24 tubes from the same population subjected to 0–10 pipetting actions to show intra-experiment variability. There are four points for each treatment but some are obscured by each other. (C) ACh produced, above that in the absence of stimulation, 1 min after; dipping a 200 μL pipette tip into the tube without sucking (×0.5) or pipetting 20 μL up and down between 1 and 50 times as shown. (n = 10). Release was significantly increased above the non-stimulated value with 1 or more pipetting actions. (D) ATP release from the same populations of cells as in (C) treated in the same way to a maximum of 100 pipetting actions.

an OCT is unlikely to be involved. $CFTR_{inh}$-172, however, an inhibitor of CFTR, which has been implicated by some in ATP release (see Discussion) did have a significant inhibitory effect on ACh release, reducing it to 68 ± 3 % of control ($P < 0.0001$, n = 20, and see Figure 4C). The IC_{50} value for this effect was 4.2 ± 0.4 μM (Figure 4D).

For comparison and to test that the drugs themselves were effective when applied to isolated cells in the way done here, their effects on stimulated ATP release were investigated, and presented in a similar way in Figure 4B. BFA, carbenoxolone and $CFTR_{inh}$-172 all significantly reduced ATP release (Figure 4B).

CFTR immuno-staining was detected in all layers of the urothelium and was highest in the outer, umbrella cell layer (Figure 5A). This contrasted with that of CK20, which was highest in the basal layer (Figure 5B).

Muscarinic receptor activation and inhibition

To determine whether muscarinic receptor activation affects ATP release, the muscarinic agonist carbachol was applied. This caused a significant increase in the amount of stimulated ATP release to 137 ± 11% (P = 0.007, n = 18) of the control (Figure 6A). Inhibition of muscarinic receptors with either 4-DAMP or methoctramine had the opposite affect and reduced ATP release to 90 ± 3 % (P = 0.03, n = 7) and 76 ± 7% (P = 0.005, n = 12) of the control respectively (Figure 6A). Greater inhibition was seen with the M_2-selective antagonist methoctramine than the M_3-selective antagonist 4-DAMP. In the presence of methoctramine, carbachol was no longer stimulatory supporting the hypothesis that the stimulation by carbachol was via an effect on muscarinic receptors. The pIC_{50} values for inhibition by methoctramine was 6.60 ± 0.25 (n = 5) (Figure 6B).

Discussion and conclusions

This is the first study to measure transmitter release from freshly isolated urothelial cells, an approach that complements existing whole tissue and cultured cell techniques but represents a more physiological experimental condition. The imposed stress used here was reproducible and not harmful,

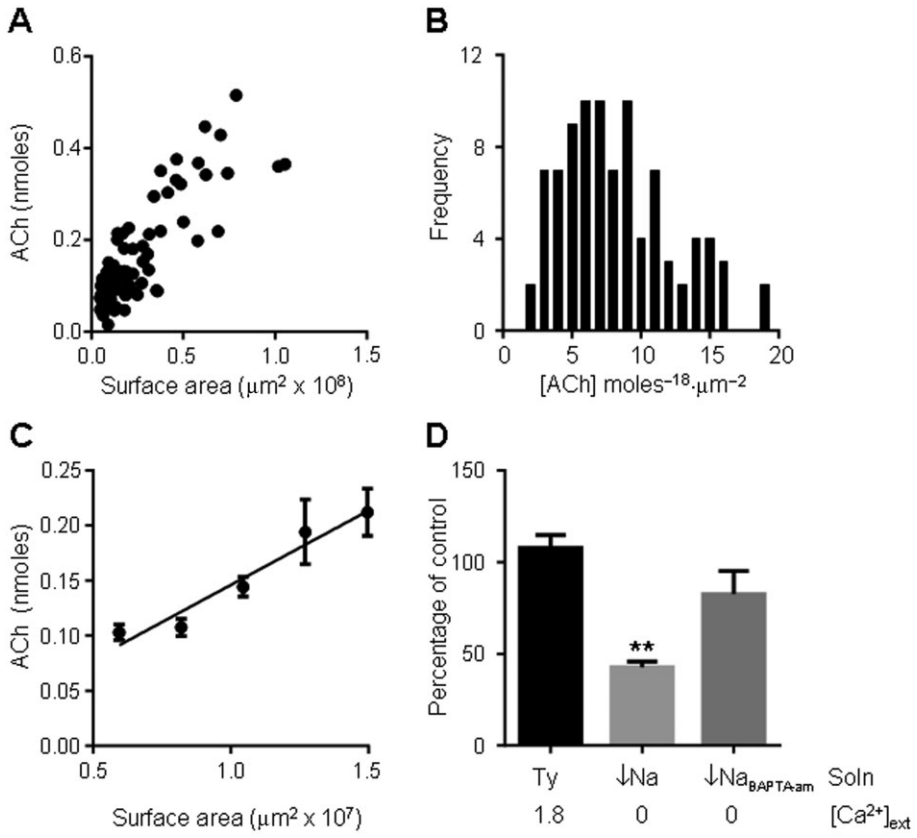

Figure 3

ACh release as a function of cell density. (A) ACh release as a function of total membrane surface area in 45 μL of cell suspension from different populations. All populations were a mixture of the three cell groups in varying proportions. Surface area was calculated assuming cells were spherical with diameters from the fits in Figure 1B as given in the text. (B) Same data as in A, but plotted as a frequency histogram of the ACh release per unit square micrometer of surface area in the tube. (C) ACh production as a function of the membrane area of the two smaller populations of cells (basal and intermediate) from a single isolation with constant larger (umbrella) cell number ($2.25 \times 10^4 \cdot mL^{-1}$) but varying total cell number. (D) Stimulated ACh as a percentage of its own paired Tyrode's solution control with no added external calcium. The bars show, respectively, Tyrode's solution with 1.8 mM extracellular calcium added (no significant effect on ACh release), low sodium Tyrode's solution, which has been shown to increase intracellular calcium (ACh release was significantly reduced to 43 ± 3% of the control $P = 0.0001$, $n = 11$) and this low sodium Tyrode's solution with BAPTA-AM, which reversed the effect of the low sodium treatment (not significantly different to Tyrode's control, $n = 6$).

and by producing a large number of equivalent tubes of cell suspension, drug application studies and comparisons between ACh and ATP were possible in the same populations of cells. Five pipetting stimuli were used rather than one to remove any variability between tubes by guaranteeing maximal ACh release. The total amount of ACh released equates to about 3 μmoles·g^{-1} of cells (assuming a specific density of 1 g·cm^{-3} and spherical cells) and is considerably higher than that reported elsewhere (Yoshida *et al.*, 2004; Lips *et al.*, 2007). This is not unexpected for several reasons: the stimulus was maximal; the small volumes possible with this technique allow more accurate measurements; the fact that the cells are dissociated permits ACh release over their entire surface area; total released ACh is measured, as the assay measures choline and so is independent of any choline esterase activity that may be present.

Of significance was the small dynamic range for ACh release. By comparison with ATP release, it is clear that this is not simply due to the technique but a real difference between the two transmitters and suggests a low threshold mechanism for ACh release, whereby it is the occurrence of a stretch rather than its magnitude that is communicated. Because cholinergic agonists increased ATP release, we propose that urothelial ACh release acts as a baseline regulator of ATP release, that is, ACh release alters the gain of the graded release of ATP with differing strengths of physical stimuli. Reduction of ACh release – for example, through M_2-receptor antagonism – would reduce the sensitivity of the stress-mediated release of ATP.

We investigated the effects of $CFTR_{inh}$-172 on ACh and ATP release because CFTR has been previously implicated in ATP release in a range of different cell types (Reisin *et al.*, 1994; Schwiebert *et al.*, 1995; Jiang *et al.*, 1998; Reigada and Mitchell, 2005; Ruan *et al.*, 2012), although not in all (Reddy *et al.*, 1996; Grygorczyk and Hanrahan, 1997; Watt *et al.*, 1998; Hazama *et al.*, 1999; Donaldson *et al.*, 2000; Okada *et al.*, 2006). The IC_{50} value for $CFTR_{inh}$-172 inhibition of ACh release is 10-fold higher than reported in epithelial cells (Ma

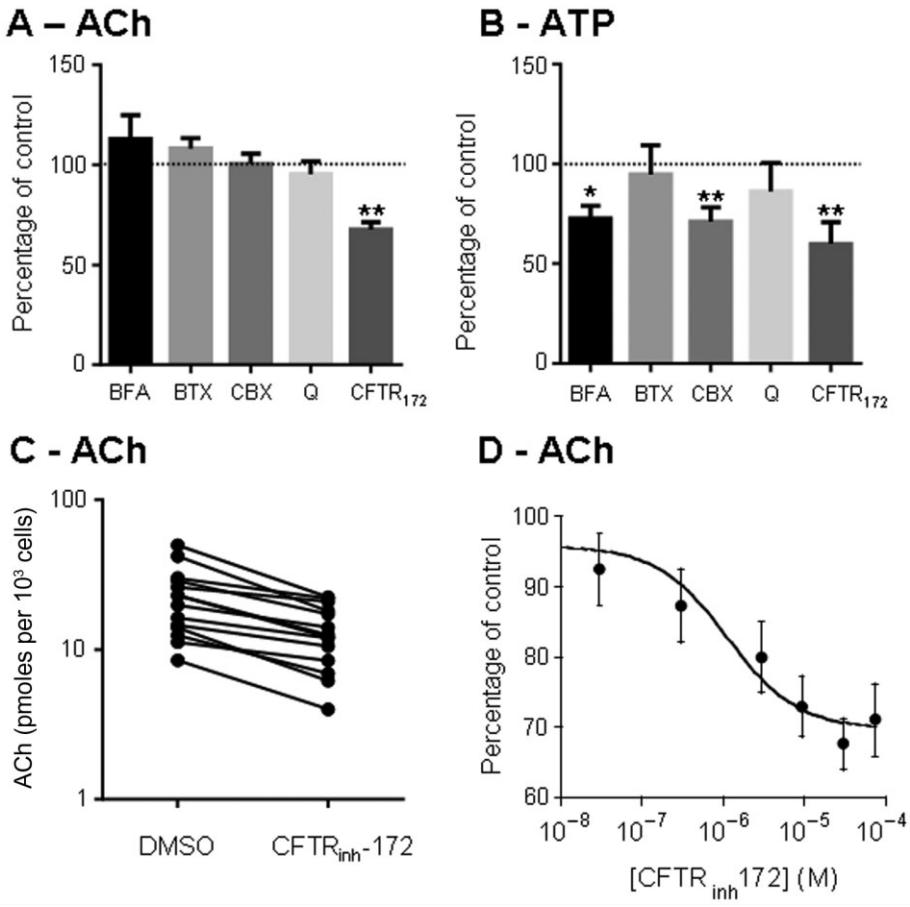

Figure 4

Analysis of the mechanism of ACh release. (A) BFA (10^{-5} g·mL^{-1}, $n = 14$), BTX (4U or 10U, $n = 7$), carbenoxolone (CBX; 5×10^{-4} M, $n = 6$) or quinine (Q; 10^{-4} M, $n = 12$) did not affect ACh production. Only the $CFTR_{inh}$-172 ($CFTR_{172}$, 3×10^{-5} M, $n = 20$, $P < 0.0001$) depressed ACh production. (B) Corresponding data for ATP release with the same drug concentrations, illustrating a significant decrease in ATP release with BFA ($n = 12$, $P = 0.015$), CBX ($n = 13$, $P = 0.0074$) and $CFTR_{inh}$-172 ($n = 8$, $P = 0.004$). (C) Paired control (DMSO) and $CFTR_{inh}$-172-treated populations showing the decrease in stimulated ACh on application of $CFTR_{inh}$-172 in more detail. (D) Dose-response curve for inhibition of ACh production by $CFTR_{inh}$-172. (IC_{50} value = 4.2 ± 0.4 $\times 10^{-6}$ M).

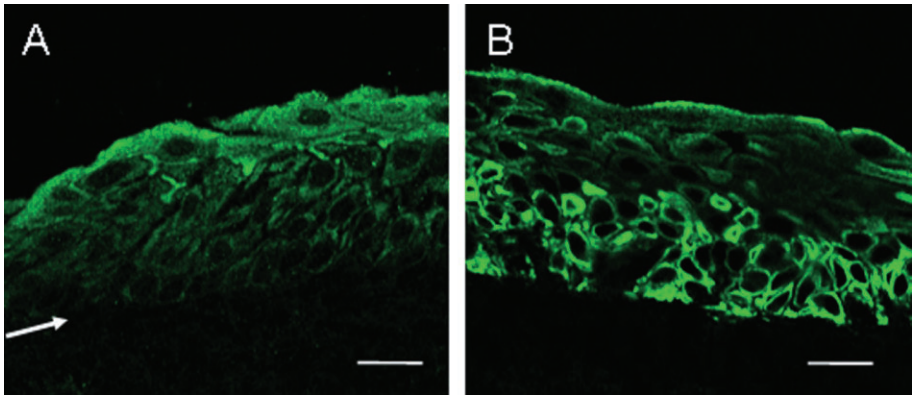

Figure 5

Distribution of CFTR and CK20 labelling in the bladder urothelium. (A) Staining with anti-CFTR antibody, showing greatest labelling in the outer, umbrella cell layer. Arrow indicates the lamina propria, the barrier between the urothelium and sub-urothelium. (B) Similar section labelled with the CK20 antibody, showing highest labelling in the basal cell layer. Bars are 25 μm.

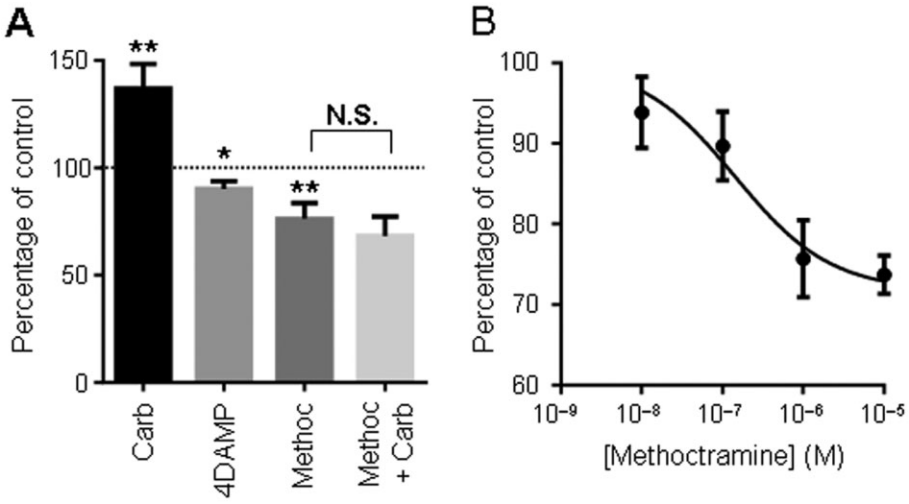

Figure 6

Muscarinic receptor activation affects ATP release. (A) ATP release following shear stress ×50, in the presence of carbachol (Carb, 10^{-5} M, to 137 ± 11% control, $P = 0.007$, $n = 18$, one outlier was omitted as ATP release was much greater than the rest), 4-DAMP (5×10^{-7} M, to 90 ± 3% of control, $P = 0.026$, $n = 7$), methoctramine (Methoc, 10^{-5} M, to 76 ± 7% control, $P = 0.005$, $n = 12$) and methoctramine and carbachol (methoc + carb, 68 ± 9%, $n = 5$), each expressed as a percentage of the corresponding control. (B) Dose-dependent inhibition of ATP release by methoctramine, expressed as a percentage of DMSO control in the absence of drug.

et al., 2002) but similar to 3.5 μM found for ATP inhibition in cultured retinal pigment epithelial cells (Reigada and Mitchell, 2005). CFTR mRNA has been detected in pig bladder tissue by reverse-transcription PCR (Plog *et al.*, 2010) and the immunohistochemistry results presented here indicate that CFTR protein is expressed within the urothelium. Although CFTR has been linked to ATP release in a number of cell types, it is unlikely to have caused the effects on ACh as both BFA and carbenoxolone reduced ATP without affecting ACh release. The selectivity of CFTR for anions over cations is only about 10-fold (Anderson *et al.*, 1991) and the pore is relatively large (Linsdell and Hanrahan, 1998) so it is possible that ACh could pass directly through the CFTR channel, either alone or with some cofactor. It is also possible that CFTR could affect ACh storage and thereby the amount available. This is suggested by cystic fibrosis patients who have a 70% reduced ACh content in lung tissue and leucocytes (Wessler *et al.*, 2007; Innis *et al.*, 2011) and the colocalization of CFTR and choline acetyltransferase in leucocytes (Wessler *et al.*, 2007). A role in choline transport is also possible as cystic fibrosis patients have reduced plasma choline levels (Innis *et al.*, 2011).

The absence of an effect of BTX on non-neuronal ACh release is consistent with a non-vesicular pathway and a different mechanism from that for neuronal ACh release. It is possible however that BTX is unable to enter the urothelial cells as botulinum injections have greater efficacy than intravesical application (Smith *et al.*, 2008) and synaptic vesicle protein SV2 used for internalization is difficult to identify in urothelial cells (Dong *et al.*, 2006; Coelho *et al.*, 2010) as are cleaved fragments of SNAP 25 that represent the target for intracellular BTX (Coelho *et al.*, 2012).

Anti-muscarinic drugs are the primary treatment for overactive bladder and were introduced as it was presumed that they would antagonize muscarinic receptors on detrusor smooth muscle, thus shielding them from excessive release of ACh from parasympathetic efferents. Identification of the M_3 subtype as the functional muscarinic receptor (Chess-Williams *et al.*, 2001) stimulated the manufacture of M_3 receptor-specific antagonists for overactive bladder, such as darifenacin (Haab *et al.*, 2004). This paradigm has been questioned as anti-muscarinic antagonists seem to be more effective during bladder filling (Finney *et al.*, 2006) than emptying, when parasympathetic activity would be low and the M_3 receptor-selective agents did not show greater efficacy compared with non-selective M_2/M_3 agents (Chapple *et al.*, 2008). These data provide at least a partial explanation for these observations: urothelial ACh release occurs during filling via an M_2 receptor-selective pathway and anti-muscarinic agents may act on this pathway within the micturition cycle. Although both 4-DAMP (M_3 receptor selective) and methoctramine (M_2 receptor selective) reduced ACh release, methoctramine caused the larger reduction. Although the pIC_{50} value for inhibition by methoctramine is high compared with its binding constant to the M_2 receptor, 4-DAMP had little effect even at very high concentrations. Instead, they may both may be acting at M_2 receptors but with reduced sensitivity.

The effect of modulating muscarinic receptors on ATP release suggests that by inhibiting ACh release, the $CFTR_{inh}$-172 could reduce ATP release indirectly, although a direct route cannot be ruled out. Either way, inhibition of CFTR offers an exciting new target for the treatment of overactive bladder.

In conclusion, pressure on isolated urothelial cells caused ACh release from urothelial cells by a route different from that for ATP and involving CFTR. It is hypothesized that this ACh may control ATP release and thus contributes to the action of anti-muscarinic agents to reduce lower urinary tract symptoms (LUTS) through attenuation of sensory afferent

pathways. Additionally, the identification of an involvement of CFTR in ACh release offers the exciting new possibility of targeting CFTR, as part of a multi-drug approach, in the treatment of lower urinary tract disorders.

Acknowledgements

We would like to thank INComb for funding this work as part of a joint EU FP7 grant and acknowledge and thank Allergan Pharmaceuticals Ireland for the supply of Onabotulinumtoxin A. J. S. Young was supported by the Rosetrees Trust and the Research into Ageing Fund, a fund set up and managed by Age UK.

Author contributions

Study concept and design: McLatchie, Young and Fry. Acquisition of data: McLatchie. Analysis and interpretation of data: McLatchie and Fry. Drafting of manuscript: McLatchie. Critical review of manuscript: Young and Fry. Statistical analysis: McLatchie and Fry. Funding: Fry.

Conflict of interests

Prof. Chris Fry is a consultant for Eli-Lilly.

References

Alexander SPH, Benson HE, Faccenda E, Pawson AJ, Sharman JL, McGrath JC *et al*. (2013). The concise guide to pharmacology 2013/14: overview. Br J Pharmacol 170: 1449–1458.

Anderson MP, Gregory RJ, Thompson S, Souza DW, Paul S, Mulligan RC *et al*. (1991). Demonstration that Cftr is a chloride channel by alteration of its anion selectivity. Science 253: 202–205.

Andersson KE (2011). Antimuscarinic mechanisms and the overactive detrusor: an update. Eur Urol 59: 377–386.

Beckel JM, Kanai A, Lee SJ, de Groat WC, Birder LA (2006). Expression of functional nicotinic acetylcholine receptors in rat urinary bladder epithelial cells. Am J Physiol-Renal 290: F103–F110.

Chapple CR, Khullar V, Gabriel Z, Muston D, Bitoun CE, Weinstein D (2008). The effects of antimuscarinic treatments in overactive bladder: an update of a systematic review and meta-analysis. Eur Urol 54: 543–562.

Chess-Williams R, Chapple CR, Yamanishi T, Yasuda K, Sellers DJ (2001). The minor population of M-3-receptors mediate contraction of human detrusor muscle in vitro. J Auton Pharmacol 21: 243–248.

Coelho A, Dinis P, Pinto R, Gorgal T, Silva C, Silva A *et al*. (2010). Distribution of the high-affinity binding site and intracellular target of botulinum toxin type A in the human bladder. Eur Urol 57: 884–890.

Coelho A, Cruz F, Cruz CD, Avelino A (2012). Spread of onabotulinumtoxina after bladder injection. Experimental study using the distribution of cleaved SNAP-25 as the marker of the toxin action. Eur Urol 61: 1178–1184.

Donaldson SH, Lazarowski ER, Picher M, Knowles MR, Stutts MJ, Boucher RC (2000). Basal nucleotide levels, release, and metabolism in normal and cystic fibrosis airways. Mol Med 6: 969–982.

Dong M, Yeh F, Tepp WH, Dean C, Johnson EA, Janz R *et al*. (2006). SV2 is the protein receptor for botulinum neurotoxin A. Science 312: 592–596.

Finney SM, Andersson KE, Gillespie JI, Stewart LH (2006). Antimuscarinic drugs in detrusor overactivity and the overactive bladder syndrome: motor or sensory actions? BJU Int 98: 503–507.

Fry C, McLatchie L (2013). The function and regulation of stress-induced acetylcholine release from the bladder urothelium. Neurourol Urodynam 32: 633–634.

Grygorczyk R, Hanrahan JW (1997). CFTR-independent ATP release from epithelial cells triggered by mechanical stimuli. Am J Physiol-Cell Ph 272: C1058–C1066.

Haab F, Stewart L, Dwyer P (2004). Darifenacin, an M-3 selective receptor antagonist, is an effective and well-tolerated once-daily treatment for overactive bladder. Eur Urol 45: 420–429.

Hanna-Mitchell AT, Beckel JM, Barbadora S, Kanai AJ, de Groat WC, Birder LA (2007). Non-neuronal acetylcholine and urinary bladder urothelium. Life Sci 80: 2298–2302.

Hazama A, Shimizu T, Ando-Akatsuka Y, Hayashi S, Tanaka S, Maeno E *et al*. (1999). Swelling-induced, CFTR-independent ATP release from a human epithelial cell line – lack of correlation with volume-sensitive Cl(-) channels. J Gen Physiol 114: 525–533.

Innis SM, Davidson AGF, Bay BN, Slack PJ, Hasman D (2011). Plasma choline depletion is associated with decreased peripheral blood leukocyte acetylcholine in children with cystic fibrosis. Am J Clin Nutr 93: 564–568.

Jiang QS, Mak D, Devidas S, Schwiebert EM, Bragin A, Zhang YL *et al*. (1998). Cystic fibrosis transmembrane conductance regulator-associated ATP release is controlled by a chloride sensor. J Cell Biol 143: 645–657.

Kilkenny C, Browne W, Cuthill IC, Emerson M, Altman DG (2010). Animal research: Reporting *in vivo* experiments: the ARRIVE guidelines. Br J Pharmacol 160: 1577–1579.

Koepsell H, Busch A, Gorboulev V, Arndt P (1998). Structure and function of renal organic cation transporters. News Physiol Sci 13: 11–16.

Kullmann FA, Artim D, Beckel J, Barrick S, de Groat WC, Birder LA (2008). Heterogeneity of muscarinic receptor-mediated Ca(2+) responses in cultured urothelial cells from rat. Am J Physiol-Renal 294: F971–F981.

Linsdell P, Hanrahan JW (1998). Adenosine triphosphate-dependent asymmetry of anion permeation in the cystic fibrosis transmembrane conductance regulator chloride channel. J Gen Physiol 111: 601–614.

Lips KS, Volk C, Schmitt BM, Pfeil U, Arndt P, Miska D *et al*. (2005). Polyspecific cation transporters mediate luminal release of acetylcholine from bronchial epithelium. Am J Resp Cell Mol 33: 79–88.

Lips KS, Wunsch J, Zarghooni S, Bschleipfer T, Schukowski K, Weidner W *et al*. (2007). Acetylcholine and molecular components of its synthesis and release machinery in the urothelium. Eur Urol 51: 1042–1053.

McGrath J, Drummond G, McLachlan E, Kilkenny C, Wainwright C (2010). Guidelines for reporting experiments involving animals: the ARRIVE guidelines. Br J Pharmacol 160: 1573–1576.

Ma TH, Thiagarajah JR, Yang H, Sonawane ND, Folli C, Galietta LJV *et al*. (2002). Thiazolidinone CFTR inhibitor identified by high-throughput screening blocks cholera toxin-induced intestinal fluid secretion. J Clin Invest 110: 1651–1658.

Okada SF, Nicholas RA, Kreda SM, Lazarowski ER, Boucher RC (2006). Physiological regulation of ATP release at the apical surface of human airway epithelia. J Biol Chem 281: 22992–23002.

Plog S, Mundhenk L, Bothe MK, Klymiuk N, Gruber AD (2010). Tissue and cellular expression patterns of porcine CFTR: similarities to and differences from human CFTR. J Histochem Cytochem 58: 785–797.

Reddy MM, Quinton PM, Haws C, Wine JJ, Grygorczyk R, Tabcharani JA *et al*. (1996). Failure of the cystic fibrosis transmembrane conductance regulator to conduct ATP. Science 271: 1876–1879.

Reigada D, Mitchell CH (2005). Release of ATP from retinal pigment epithelial cells involves both CFTR and vesicular transport. Am J Physiol-Cell Ph 288: C132–C140.

Reisin IL, Prat AG, Abraham EH, Amara JF, Gregory RJ, Ausiello DA *et al*. (1994). The cystic-fibrosis transmembrane conductance regulator is a dual ATP and chloride channel. J Biol Chem 269: 20584–20591.

Ruan YC, Shum WWC, Belleannee C, Da Silva N, Breton S (2012). ATP secretion in the male reproductive tract: essential role of CFTR. J Physiol-London 590: 4209–4222.

Schwiebert EM, Egan ME, Hwang TH, Fulmer SB, Allen SS, Cutting GR *et al*. (1995). Cftr regulates outwardly rectifying chloride channels through an autocrine mechanism involving ATP. Cell 81: 1063–1073.

Smith CP, Gangitano DA, Munoz A, Salas NA, Boone TB, Aoki KR *et al*. (2008). Botulinum toxin type A normalizes alterations in urothelial ATP and NO release induced by chronic spinal cord injury. Neurochem Int 52: 1068–1075.

Watt WC, Lazarowski ER, Boucher RC (1998). Cystic fibrosis transmembrane regulator-independent release of ATP – Its implications for the regulation of P2Y(2) receptors in airway epithelia. J Biol Chem 273: 14053–14058.

Wessler I, Roth E, Deutsch C, Brockerhoff P, Bittinger F, Kirkpatrick CJ *et al*. (2001). Release of non-neuronal acetylcholine from the isolated human placenta is mediated by organic cation transporters. Brit J Pharmacol 134: 951–956.

Wessler I, Bittinger F, Kamin W, Zepp F, Meyer E, Schad A *et al*. (2007). Dysfunction of the non-neuronal cholinergic system in the airways and blood cells of patients with cystic fibrosis. Life Sci 80: 2253–2258.

Woodman JR, Mansfield KJ, Lazzaro VA, Lynch W, Burcher E, Moore KH (2011). Immunocytochemical characterisation of cultures of human bladder mucosal cells. BMC Urol 11: 5.

Yoshida M, Miyamae K, Iwashita H, Otani M, Inadome A (2004). Management of detrusor dysfunction in the elderly: changes in acetylcholine and adenosine triphosphate release during aging. Urology 63: 17–23.

Yoshida M, Inadome A, Maeda Y, Satoji Y, Masunaga K, Sugiyama Y *et al*. (2006). Non-neuronal cholinergic system in human bladder urothelium. Urology 67: 425–430.

Young JS, Matharu R, Carew MA, Fry CH (2012). Inhibition of stretching-evoked ATP release from bladder mucosa by anticholinergic agents. BJU Int 110 (8B): E397–E401.

Supporting information

Additional Supporting Information may be found in the online version of this article at the publisher's web-site:

http://dx.doi.org/10.1111/bph.12682

Appendix S1 Estimation of the drag force on an isolated cell.